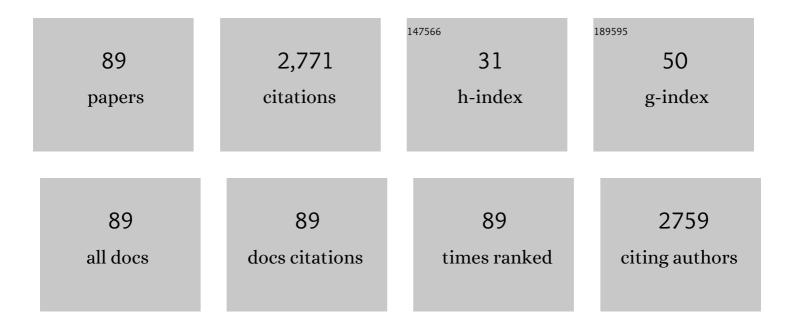
## Liliana de Campo

List of Publications by Year in descending order

Source: https://exaly.com/author-pdf/9478948/publications.pdf Version: 2024-02-01



#	Article	IF	CITATIONS
1	Tracking the heat-triggered phase change of polydopamine-shelled, perfluorocarbon emulsion droplets into microbubbles using neutron scattering. Journal of Colloid and Interface Science, 2022, 607, 836-847.	5.0	8
2	Effect of NaCl and CaCl2 concentration on the rheological and structural characteristics of thermally-induced quinoa protein gels. Food Hydrocolloids, 2022, 124, 107350.	5.6	42
3	Polycation radius of gyration in a polymeric ionic liquid (PIL): the PIL melt is not a theta solvent. Physical Chemistry Chemical Physics, 2022, 24, 4526-4532.	1.3	5
4	Small-angle X-ray scattering (SAXS) and small-angle neutron scattering (SANS) study on the structure of sodium caseinate in dispersions and at the oil-water interface: Effect of calcium ions. Food Structure, 2022, 32, 100276.	2.3	10
5	Structure–Performance Relationships for Tail Substituted Zwitterionic Betaine–Azobenzene Surfactants. Langmuir, 2022, 38, 7522-7534.	1.6	3
6	How to avoid multiple scattering in strongly scattering SANS and USANS samples. Fuel, 2022, 325, 124957.	3.4	6
7	Exploring the transition of polydopamine-shelled perfluorohexane emulsion droplets into microbubbles using small- and ultra-small-angle neutron scattering. Physical Chemistry Chemical Physics, 2021, 23, 9843-9850.	1.3	7
8	Structural evolution of iron forming iron oxide in a deep eutectic-solvothermal reaction. Nanoscale, 2021, 13, 1723-1737.	2.8	14
9	Design and synthesis of an azobenzene–betaine surfactant for photo-rheological fluids. Journal of Colloid and Interface Science, 2021, 594, 669-680.	5.0	17
10	Pore accessibility and trapping of methane in Marcellus Shale. International Journal of Coal Geology, 2021, 248, 103850.	1.9	18
11	Small-angle neutron scattering reveals basis for composition dependence of gel behaviour in oleic acid - sodium oleate oleogels. Innovative Food Science and Emerging Technologies, 2021, 73, 102763.	2.7	6
12	Deformation of pores in response to uniaxial and hydrostatic stress cycling in Marcellus Shale: Implications for gas recovery. International Journal of Coal Geology, 2021, 248, 103867.	1.9	9
13	Accessibility of Pores to Methane in New Albany Shale Samples of Varying Maturity Determined Using SANS and USANS. Energies, 2021, 14, 8438.	1.6	5
14	<i>In Situ</i> Nanostructural Analysis of Concentrated Wormlike Micellar Fluids Comprising Sodium Laureth Sulfate and Cocamidopropyl Betaine Using Small-Angle Neutron Scattering. Langmuir, 2020, 36, 14296-14305.	1.6	7
15	Determining the Hydration in the Hydrophobic Layer of Permeable Polymer Vesicles by Neutron Scattering. Macromolecules, 2020, 53, 7546-7551.	2.2	6
16	Effect of red blood cell shape changes on haemoglobin interactions and dynamics: a neutron scattering study. Royal Society Open Science, 2020, 7, 201507.	1.1	6
17	Structural Polymorphism of Resorcinarene Assemblies. Langmuir, 2020, 36, 6222-6227.	1.6	5
18	Effect of porous waxy rice starch addition on acid milk gels: Structural and physicochemical functionality. Food Hydrocolloids, 2020, 109, 106092.	5.6	7

#	Article	IF	CITATIONS
19	Self-Assembly of Surfactin into Nanofibers with Hydrophilic Channels in Nonpolar Organic Media. Langmuir, 2020, 36, 7627-7633.	1.6	3
20	Biomimetic Gemcitabine–Lipid Prodrug Nanoparticles for Pancreatic Cancer. ChemPlusChem, 2020, 85, 1283-1291.	1.3	12
21	Tunable Biomimetic Hydrogels from Silk Fibroin and Nanocellulose. ACS Sustainable Chemistry and Engineering, 2020, 8, 2375-2389.	3.2	84
22	Structural relationships for the design of responsive azobenzene-based lyotropic liquid crystals. Physical Chemistry Chemical Physics, 2020, 22, 4086-4095.	1.3	8
23	Small angle neutron scattering quantifies the hierarchical structure in fibrous calcium caseinate. Food Hydrocolloids, 2020, 106, 105912.	5.6	12
24	Membrane Protein Structures in Lipid Bilayers; Small-Angle Neutron Scattering With Contrast-Matched Bicontinuous Cubic Phases. Frontiers in Chemistry, 2020, 8, 619470.	1.8	4
25	Micron-scale restructuring of gelling silica subjected to shear. Journal of Colloid and Interface Science, 2019, 533, 136-143.	5.0	3
26	Interfacial Structures of Droplet-Stabilized Emulsions Formed with Whey Protein Microgel Particles as Revealed by Small- and Ultra-Small-Angle Neutron Scattering. Langmuir, 2019, 35, 12017-12027.	1.6	22
27	PEGylation and surface functionalization of liposomes containing drug nanocrystals for cell-targeted delivery. Colloids and Surfaces B: Biointerfaces, 2019, 182, 110362.	2.5	22
28	Small Angle Neutron Scattering Study of a Gehlenite-Based Ceramic Fabricated from Industrial Waste. Solid State Phenomena, 2019, 290, 22-28.	0.3	1
29	Protein-Eye View of the in Meso Crystallization Mechanism. Langmuir, 2019, 35, 8344-8356.	1.6	9
30	Rheological and structural characterization of acidified skim milks and infant formulae made from cow and goat milk. Food Hydrocolloids, 2019, 96, 161-170.	5.6	41
31	Robust and Tunable Hybrid Hydrogels from Photo-Cross-Linked Soy Protein Isolate and Regenerated Silk Fibroin. ACS Sustainable Chemistry and Engineering, 2019, 7, 9257-9271.	3.2	44
32	Worm-like micelles and vesicles formed by alkyl-oligo(ethylene glycol)-glycoside carbohydrate surfactants: The effect of precisely tuned amphiphilicity on aggregate packing. Journal of Colloid and Interface Science, 2019, 547, 275-290.	5.0	13
33	Structure Analysis of Solid Lipid Nanoparticles for Drug Delivery: A Combined USANS/SANS Study. Particle and Particle Systems Characterization, 2019, 36, 1800359.	1.2	20
34	Evolution of the Interfacial Structure of a Catalyst Ink with the Quality of the Dispersing Solvent: A Contrast Variation Small-Angle and Ultrasmall-Angle Neutron Scattering Investigation. ACS Applied Materials & Interfaces, 2019, 11, 9934-9946.	4.0	65
35	Effect of amyloglucosidase hydrolysis on the multi-scale supramolecular structure of corn starch. Carbohydrate Polymers, 2019, 212, 40-50.	5.1	38
36	Performance and characteristics of the BILBY time-of-flight small-angle neutron scattering instrument. Journal of Applied Crystallography, 2019, 52, 1-12.	1.9	90

#	Article	IF	CITATIONS
37	Tuning the structure, thermal stability and rheological properties of liquid crystal phases via the addition of silica nanoparticles. Physical Chemistry Chemical Physics, 2019, 21, 25649-25657.	1.3	5
38	The effects of small molecule organic additives on the self-assembly and rheology of betaine wormlike micellar fluids. Journal of Colloid and Interface Science, 2019, 534, 518-532.	5.0	51
39	Nanostructure of cokes. International Journal of Coal Geology, 2018, 188, 112-120.	1.9	21
40	Investigation of the siliceous hydrogel phase formation in glass-ionomer cement paste. Physica B: Condensed Matter, 2018, 551, 287-290.	1.3	6
41	Structural evolution of photocrosslinked silk fibroin and silk fibroin-based hybrid hydrogels: A small angle and ultra-small angle scattering investigation. International Journal of Biological Macromolecules, 2018, 114, 998-1007.	3.6	35
42	Self-Assembly of Long-Chain Betaine Surfactants: Effect of Tailgroup Structure on Wormlike Micelle Formation. Langmuir, 2018, 34, 970-977.	1.6	52
43	Fingerprint of hydrocarbon generation in the southern Georgina Basin, Australia, revealed by small angle neutron scattering. International Journal of Coal Geology, 2018, 186, 135-144.	1.9	11
44	Microstructure characterisation through ultra-small-angle neutron scattering. International Journal of Nanotechnology, 2018, 15, 766.	0.1	0
45	Sulfonated Thiophene Derivative Stabilized Aqueous Poly(3-hexylthiophene):Phenyl-C <sub>61</sub> -butyric Acid Methyl Ester Nanoparticle Dispersion for Organic Solar Cell Applications. ACS Applied Materials & Interfaces, 2018, 10, 44116-44125.	4.0	18
46	H2O/D2O Contrast Variation for Ultra-Small-Angle Neutron Scattering to Minimize Multiple Scattering Effects of Colloidal Particle Suspensions. Colloids and Interfaces, 2018, 2, 37.	0.9	20
47	Structural and rheological changes of lamellar liquid crystals as a result of compositional changes and added silica nanoparticles. Physical Chemistry Chemical Physics, 2018, 20, 16592-16603.	1.3	15
48	Wormlike micelle formation of novel alkyl-tri(ethylene glycol)-glucoside carbohydrate surfactants: Structure–function relationships and rheology. Journal of Colloid and Interface Science, 2018, 529, 464-475.	5.0	38
49	Design and performance of the variable-wavelength Bonse–Hart ultra-small-angle neutron scattering diffractometer KOOKABURRA at ANSTO. Journal of Applied Crystallography, 2018, 51, 1-8.	1.9	68
50	Tough Photocrosslinked Silk Fibroin/Graphene Oxide Nanocomposite Hydrogels. Langmuir, 2018, 34, 9238-9251.	1.6	54
51	Bulk properties of aqueous graphene oxide and reduced graphene oxide with surfactants and polymers: adsorption and stability. Physical Chemistry Chemical Physics, 2018, 20, 16801-16816.	1.3	41
52	Rearrangement in Brown Coal Microstructure upon Drying As Measured by Ultrasmall-Angle Neutron Scattering. Energy & Fuels, 2017, 31, 231-238.	2.5	6
53	Optimal packings of three-arm star polyphiles: from tricontinuous to quasi-uniformly striped bicontinuous forms. Interface Focus, 2017, 7, 20160130.	1.5	6
54	Towards advanced paramagnetic nanoassemblies of highly ordered interior nanostructures as potential MRI contrast agents. New Journal of Chemistry, 2017, 41, 2735-2744.	1.4	4

#	Article	IF	CITATIONS
55	Crystallographic characterization of fluorapatite glass-ceramics synthesized from industrial waste. Powder Diffraction, 2017, 32, S61-S65.	0.4	3
56	Polymeric Ionic Liquid Nanoparticle Emulsions as a Corrosion Inhibitor in Anticorrosion Coatings. ACS Omega, 2016, 1, 29-40.	1.6	31
57	Investigation of the micro- and nano-scale architecture of cellulose hydrogels with plant cell wall polysaccharides: A combined USANS/SANS study. Polymer, 2016, 105, 449-460.	1.8	31
58	KOOKABURRA: The Ultra-Small-Angle Neutron Scattering Instrument at ANSTO. Neutron News, 2016, 27, 30-32.	0.1	7
59	Structural Evolution of Wormlike Micellar Fluids Formed by Erucyl Amidopropyl Betaine with Oil, Salts, and Surfactants. Langmuir, 2016, 32, 12423-12433.	1.6	39
60	Using SANS with Contrast-Matched Lipid Bicontinuous Cubic Phases To Determine the Location of Encapsulated Peptides, Proteins, and Other Biomolecules. Journal of Physical Chemistry Letters, 2016, 7, 2862-2866.	2.1	23
61	BILBY: Time-of-Flight Small Angle Scattering Instrument. Neutron News, 2016, 27, 9-13.	0.1	59
62	Gdâ€DTPAâ€Dopamineâ€Bisphytanyl Amphiphile: Synthesis, Characterisation and Relaxation Parameters of the Nanoassemblies and Their Potential as MRI Contrast Agents. Chemistry - A European Journal, 2015, 21, 13950-13960.	1.7	12
63	Investigating linear and nonlinear viscoelastic behaviour and microstructures of gelatin-multiwalled carbon nanotube composites. RSC Advances, 2015, 5, 107916-107926.	1.7	21
64	Nanocompartmentalization of Soft Materials with Three Mutually Immiscible Solvents: Synthesis and Self-Assembly of Three-Arm Star-Polyphiles. Chemistry of Materials, 2015, 27, 857-866.	3.2	8
65	Evaluation of Gd-DTPA-Monophytanyl and Phytantriol Nanoassemblies as Potential MRI Contrast Agents. Langmuir, 2015, 31, 1556-1563.	1.6	16
66	Chemical delithiation and exfoliation of <mml:math xmlns:mml="http://www.w3.org/1998/Math/MathML" altimg="si0033.gif" overflow="scroll"&gt;<mml:msub><mml:mrow><mml:mi>Li</mml:mi></mml:mrow><mml:mi>xJournal of Solid State Chemistry, 2014, 220, 102-110.</mml:mi></mml:msub></mml:math 	n1.4 mi>₹/mm	l:mrow>
67	The Tricontinuous 3ths(5) Phase: A New Morphology in Copolymer Melts. Macromolecules, 2014, 47, 7424-7430.	2.2	11
68	Nanoassemblies of Gd–DTPA–monooleyl and glycerol monooleate amphiphiles as potential MRI contrast agents. Journal of Materials Chemistry B, 2014, 2, 1225.	2.9	25
69	Gadolinium-DTPA amphiphile nanoassemblies: agents for magnetic resonance imaging and neutron capture therapy. Biomaterials Science, 2014, 2, 924-935.	2.6	24
70	Hierarchical self-assembly of a striped gyroid formed by threaded chiral mesoscale networks. Proceedings of the National Academy of Sciences of the United States of America, 2014, 111, 1271-1276.	3.3	40
71	Polycontinuous geometries for inverse lipid phases with more than two aqueous network domains. Faraday Discussions, 2013, 161, 215-247.	1.6	35
72	Minimal nets and minimal minimal surfaces. Acta Crystallographica Section A: Foundations and Advances, 2013, 69, 483-489.	0.3	13

#	Article	IF	CITATIONS
73	Influence of Vitamin E Acetate and Other Lipids on the Phase Behavior of Mesophases Based on Unsaturated Monoglycerides. Langmuir, 2013, 29, 8222-8232.	1.6	42
74	Texture Effects in the Delithiation of Lithium Cobalt Oxide. Materials Science Forum, 2012, 736, 301-306.	0.3	0
75	Chelating DTPA amphiphiles: ion-tunable self-assembly structures and gadolinium complexes. Physical Chemistry Chemical Physics, 2012, 14, 12854.	1.3	13
76	A novel lyotropic liquid crystal formed by triphilic star-polyphiles: hydrophilic/oleophilic/fluorophilic rods arranged in a 12.6.4. tiling. Physical Chemistry Chemical Physics, 2011, 13, 3139-3152.	1.3	36
77	Chelating oleyl-EDTA amphiphiles: self-assembly, colloidal particles, complexation with paramagnetic metal ions and promise as magnetic resonance imaging contrast agents. Soft Matter, 2011, 7, 10994.	1.2	31
78	A Bicontinuous Mesophase Geometry with Hexagonal Symmetry. Langmuir, 2011, 27, 10475-10483.	1.6	19
79	Chelating phytanyl-EDTA amphiphiles: self-assembly and promise as contrast agents for medical imaging. Soft Matter, 2010, 6, 5915.	1.2	41
80	Tricontinuous mesophases of balanced three-arm â€~star polyphiles'. Soft Matter, 2009, 5, 2782.	1.2	35
81	Formation and Characterization of Emulsified Microemulsions. Surfactant Science, 2008, , .	0.0	2
82	An attempt to detect bicontinuity from SANS data. Journal of Colloid and Interface Science, 2007, 312, 59-67.	5.0	16
83	Oil-Loaded Monolinolein-Based Particles with Confined Inverse Discontinuous Cubic Structure (Fd3m). Langmuir, 2006, 22, 517-521.	1.6	162
84	Control of the Internal Structure of MLO-Based Isasomes by the Addition of Diglycerol Monooleate and Soybean Phosphatidylcholine. Langmuir, 2006, 22, 9919-9927.	1.6	125
85	Crystallography of dispersed liquid crystalline phases studied by cryo-transmission electron microscopy. Journal of Microscopy, 2006, 221, 110-121.	0.8	117
86	Emulsified Microemulsions and Oil-Containing Liquid Crystalline Phases. Langmuir, 2005, 21, 569-577.	1.6	241
87	Five-component food-grade microemulsions: structural characterization by SANS. Journal of Colloid and Interface Science, 2004, 274, 251-267.	5.0	71
88	Structural characterization of five-component food grade oil-in-water nonionic microemulsions. Physical Chemistry Chemical Physics, 2004, 6, 1524-1533.	1.3	48
89	Reversible Phase Transitions in Emulsified Nanostructured Lipid Systems. Langmuir, 2004, 20, 5254-5261.	1.6	222